


FK506-binding protein 5 regulates cell quiescence-proliferation decision in zebrafish epithelium

Yingxiang Li¹, Chengdong Liu^{1,*}, Xuanxuan Bai², Mingyu Li² and Cunming Duan¹ 

1 Department of Molecular, Cellular and Developmental Biology, University of Michigan, Ann Arbor, MI, USA

2 School of Pharmaceutical Sciences, Fujian Provincial Key Laboratory of Innovative Drug Target Research, Xiamen University, China

Correspondence

C. Duan, Department of Molecular, Cellular and Developmental Biology, University of Michigan, Ann Arbor, MI 48109, USA
Tel: +734-763-4710
E-mail: cduan@umich.edu

Present address

* Key Laboratory of Mariculture (Ministry of Education), Ocean University of China, Qingdao, China

Yingxiang Li and Chengdong Liu contributed equally to this article

(Received 24 March 2023, revised 9 May 2023, accepted 15 May 2023, available online 13 June 2023)

doi:10.1002/1873-3468.14670

Edited by Didier Stainier

Using a zebrafish ionocyte model, transcriptomics and genetic analyses were performed to identify pathways and genes involved in cell quiescence-proliferation regulation. Gene ontology and Kyoto encyclopedia of genes and genomes pathway analyses revealed that genes involved in transcription regulation, cell cycle, Foxo signalling and Wnt signalling pathway are enriched among the up-regulated genes while those involved in ion transport, cell adhesion and oxidation–reduction are enriched among the down-regulated genes. Among the top up-regulated genes is FK506-binding protein 5 (Fkbp5). Genetic deletion and pharmacological inhibition of Fkbp5 abolished ionocyte reactivation and impaired Akt signalling. Forced expression of a constitutively active form of Akt rescued the defects caused by Fkbp5 inhibition. These results uncover a key role of Fkbp5 in regulating the quiescence-proliferation decision via Akt signalling.

Keywords: Akt; calcium signalling; cell cycle; FK506 binding protein 5; IGF signalling; ionocyte

The active cell cycle consists of four phases: G1, S, G2 and M. In addition, the G0 phase or quiescence phase exists outside of the proliferative cycle. Cells in the quiescence phase, while non-dividing and dormant, can re-enter the cell cycle upon injuries or receiving appropriate signals and stimuli [1]. Quiescence prevents long-lived cells (such as adult stem cells) from accumulation of genomic aberrations and stress. Dysregulation of the proliferation-quiescence balance can lead to hyper- and hypo-proliferative human diseases, including cancer and fibrosis [1].

Abbreviations

DEG, differential gene expression; FACS, fluorescence-activated cell sorting; Fkbp5, FK506-binding protein 5; GO, gene ontology; IP3Rs, inositol 1,4,5-trisphosphate receptors; KEGG, Kyoto encyclopedia of genes and genomes; RIN, RNA Integrity Number; RyRs, ryanodine receptors.

The molecular mechanisms underlying the proliferation-quiescence decision have been studied extensively using cultured cells [1]. Based on data collected from cultured mammalian cells kept in mitogen-free media for different time periods, Pardee [2] proposed that a ‘restriction’ point exists in late G1 phase [2]. Cells that have crossed this check point prior to the mitogen removal usually complete the next cell cycle. In contrast, cells that have not reached this check point at the time of mitogen removal become quiescent and enter the G0 phase. Yao *et al.* [3] showed that Rb and E2F play a critical role in regulating the proliferation-quiescence decision in cultured mammalian

cells [3]. Subsequent studies have led to the proposal of a bifurcation mechanism controlled by CDK2 and its inhibitor p21 [4]. Cells that cross this bifurcation point at the end of mitosis with high CDK2 activity enter the next active cell cycle. Those with low CDK2 activity enter the quiescence phase [4]. These *in vitro* findings have been integrated into a two-step model recently [1]. According to this model, the proliferation-quiescence decision is regulated by two bistable switches. The Rb-E2F acts as the first switch. This bistable switch integrates extracellular mitogenic signals via Cyclin D:CDK4/6 activity. The Rb-E2F switch activity is also influenced by DNA damage and metabolic signals. A second bistable switch is regulated by CDK2 activity and p21 degradation. The time between these two points represents a window for cell cycle reversibility [1]. While these findings have provided important insights into how cells exit the active cell cycle and enter the quiescence, key questions remain. To date, the molecular nature and precise position of the commitment point in the cell cycle are unknown [1]. We have a limited understanding of how quiescent cells are reactivated and re-enter the active cell cycle. Moreover, these models are developed primarily based on cell culture systems, mostly in immortalised cell lines. We now understand that there are tremendous complexities *in vivo*, ranging from crosstalk with various hormones and growth factors, the availability of local nutrients and oxygen, to various feedback loops. These complexities cannot be captured by cell culture-based assays.

We have recently discovered that a population of epithelial cells in zebrafish, known as Na⁺-K⁺-ATPase-rich ionocytes or NaR cells, are reactivated and undergo robust cell division in response to low calcium stress or genetic manipulations [5–9]. NaR cells are structurally and functionally similar to human intestinal and renal epithelial cells and contain all molecular components for transcellular Ca²⁺ transport, including the epithelial Ca²⁺ channel Trpv6. Zebrafish live in hypoosmotic aquatic habitats and use NaR cells to take up Ca²⁺ from the surrounding water to maintain their body calcium

homeostasis [10]. Under normal medium, the constitutively open Trpv6 mediates Ca²⁺ influx continuously and maintains a high level of cytoplasmic free Ca²⁺ ([Ca²⁺]_c) in these cells. The high [Ca²⁺]_c suppresses Akt-Tor signalling via the conserved protein phosphatase PP2A and promotes cell quiescence [9]. When fish are transferred to an embryo medium containing low [Ca²⁺] or when Trpv6 is genetically deleted, the [Ca²⁺]_c drops and NaR cells re-enter the cell cycle due to the re-activation of Igfbp5a-Igflr-PI3 kinase-Akt-Tor signalling pathway [5–9,11]. These findings are consistent with the known role of the AKT–mTOR signalling in reactivating adult stem cells and T cells in mammals and *Drosophila* [12–14], suggesting this is an evolutionarily conserved mechanism(s).

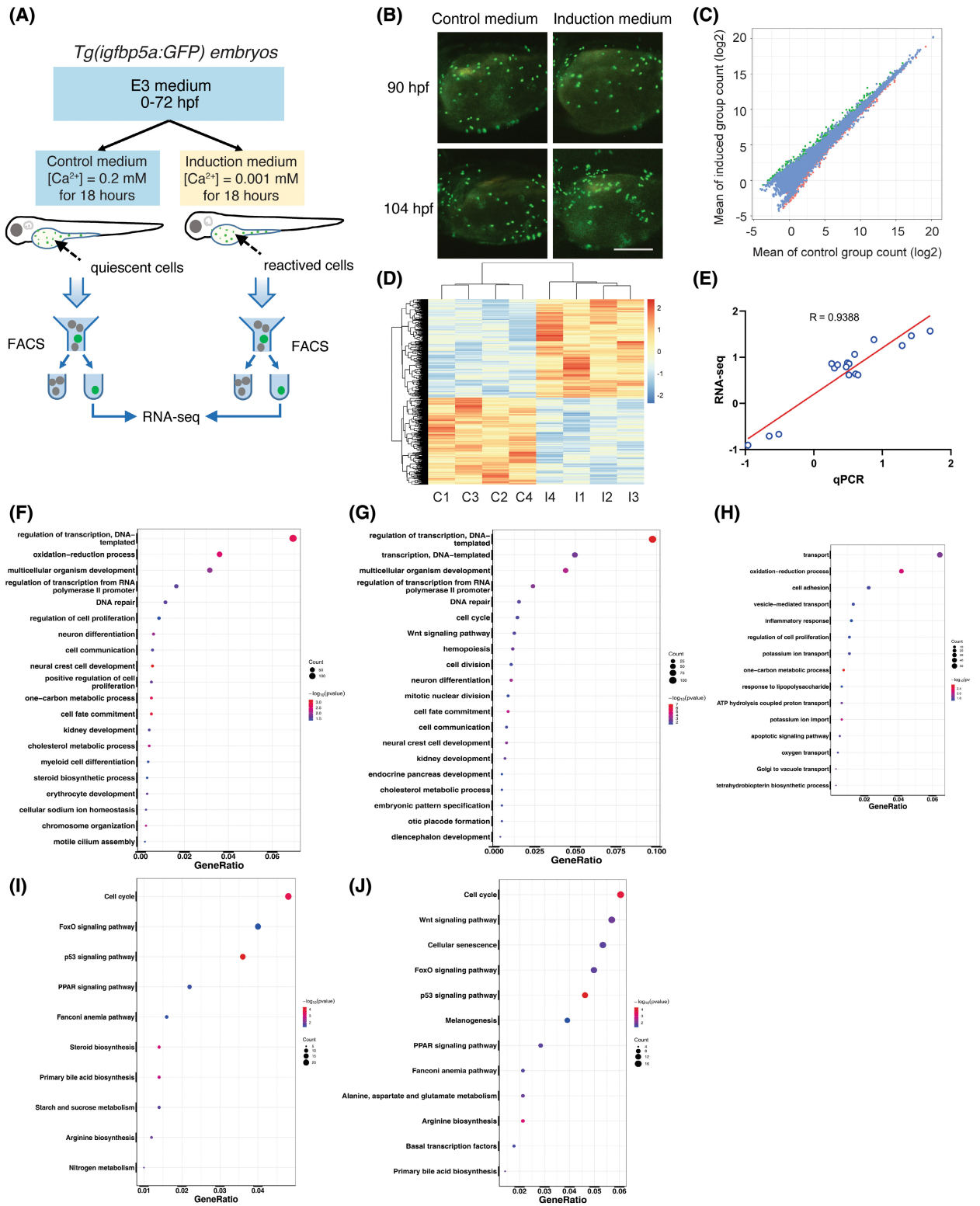
To identify pathways and molecules regulating the quiescence-proliferation transition *in vivo*, we engineered a stable zebrafish transgenic line Tg(*igfbp5a*:GFP) in which NaR cells are genetically labelled with GFP. These transgenic fish faithfully report NaR cell reactivation [7–9]. Zebrafish are oviparous vertebrates. Their free-living, tiny and transparent embryos make it a popular model organism in developmental biology. NaR cells in particular are located on the surface of yolk sac skin larval fish, making Tg(*igfbp5a*:GFP) fish well suited for *in vivo* analysis of the quiescence-proliferation regulation. RNA-seq analysis results showed that genes involved in cell cycle, gene transcription, Foxo signalling etc. are up-regulated in reactivated NaR cells while genes involved in ion transport, cell adhesion and oxidation–reduction are down-regulated. Further data mining and genetic experiments uncovered Fkbp5 as a key regulator of NaR cell quiescence-proliferation decision *in vivo*.

Results

The transcriptomic profile of reactivated NaR cells

The RNA-seq experiment design is shown in Fig. 1A. NaR cells were isolated by fluorescence-activated cell

Fig. 1. Identification and analysis of differentially expressed genes (DEGs). (A) The RNA-seq experiment design. (B) Representative images of Tg(*igfbp5a*:GFP) larvae at the indicated stages grown in the control medium or the induction medium. Shown here and in following figures are lateral views of the yolk sac region. Anterior to the left and dorsal up. Note clusters of newly divided NaR cells induced by the induction medium at 104 h post fertilisation (hpf). (C) Pairwise comparison of gene expression abundance between the control and the induced NaR cells. The up- and down-regulated genes were shown in green and red, respectively. Genes that were not changed are shown in blue. (D) Hierarchical clustering of the DEGs in the four control (C1–C4) and four induction groups (I1–I4) of NaR cells. Red colour indicates up-regulated genes and blue colour down-regulated genes. (E) qRT-PCR confirmation of RNA-seq data. Changes (log₂) in the mRNA levels of the indicated genes measured by RNA-seq were plotted against those detected by qPCR. The line indicates the linear correlation between the results of RNA-seq and qPCR. (F–H) Gene ontology (GO) analysis results of all (F), up-regulated (G) and down-regulated (H) DEGs. The dot size indicates the number of genes, and the x-axis indicates the identified genes ratio in the relevant GO term. (I, J) Kyoto encyclopedia of genes and genomes (KEGG) analysis of all (I), and up-regulated (J). The dot size indicates the number of identified genes, and the x-axis indicates the genes ratio in the relevant KEGG pathway.



sorting (FACS) sorting from *Tg(igfbp5a:GFP)* fish treated with the induction medium or control medium. RNA was isolated from these cells and subjected to

RNA-seq analysis. As reported previously [7], NaR cells in the induction medium-treated fish underwent proliferation and formed clusters of newly divided cells

in the yolk sac region while those in the control medium remained undivided (Fig. 1B). A total of 27 107 genes were detected. The genes' mapping ratios were 83.5%–88.1% (Fig. S1A,B). Differential gene expression (DEG) analysis detected a total of 2164 DEGs. Among them, 1168 genes were up-regulated and 996 were down-regulated in reactivated NaR cells (Fig. 1C; Table S1). Hierarchical clustering of DEGs showed that the reactivated NaR cell datasets clustered distinctly from the control NaR cell dataset (Fig. 1D). In agreement, principal component analysis showed that the reactivated NaR cell datasets clustered distinctly from those of the quiescent NaR cell dataset (Fig. S1C,D). To confirm the RNA-seq results, qRT-PCR assays were performed using a different set of FACS-sorted NaR cells and similar changes were detected in 17 out of the 17 genes examined (Fig. 1E; Fig. S2).

Gene ontology (GO) and Kyoto Encyclopedia of Genes and Genomes (KEGG) enrichment analysis

The identified DEGs were annotated with GO terms and sorted based on functional categories. Genes involved in transcription regulation, oxidation reduction, multicellular organism development, DNA repair and cell proliferation are enriched (Fig. 1E). When the up-regulated and down-regulated DEGs were analysed separately, genes involved in transcription/regulation, multicellular organism development, cell cycle/cell division, DNA repair and Wnt signalling are enriched in the up-regulated DEGs (Fig. 1F). Among the down-regulated genes, the most enriched GO term is transport, followed by oxidation reduction, cell adhesion and vesicle-mediated transport (Fig. 1G).

KEGG pathway enrichment analysis was performed next. The DEGs were significantly enriched in cell cycle, Foxo signalling, p53 signalling, PPAR signalling and Fanconi anaemia pathway (Fig. 1H). These pathways were also enriched in the up-regulated DEGs (Fig. 1I). Additionally, Wnt signalling, cellular senescence and melanogenesis genes were also enriched (Fig. 1I). The enrichment of up-regulated 'cell cycle' genes is in good agreement with the fact that these are rapidly dividing cells. Although KEGG analysis suggested an enrichment of the p53 signalling and cell senescence pathways (Fig. 1H,I), many of the genes are overlapping with those in the cell-cycle pathway (Fig. S3). Genes in this category include *cdk21*, *gad45aa*, *ccne2*, *cdkn1a*, *cenb2*, *ccnd1*, *chek1* and *e2f2* (Fig. S3). There are also significant overlaps in the Wnt and melanogenesis pathways (Fig. S5), including *wnt7ba*, *wnt8b*, *wnt 11*, *wnt6b*, *wnt7bb* and *wnt7aa*,

consistent with the role of Wnt signalling in regulating melanocyte development [15].

Fkbp5 is up-regulated and is indispensable in NaR cell reactivation

We mined the RNA-seq dataset further by ranking the up-regulated DEGs based on their relative mRNA abundance in NaR cells (Table 1). As expected, the calcium channel gene *trpv6*, which has been shown to regulate NaR cell proliferation-quiescence decision by suppressing the Igf1r-PI3 kinase-Akt-Tor signalling pathway [9], is among this group. Others are *col2a1a*, *caspb*, *her9*, *ankhb*, *pck1*, *fkbp5*, *si:dkey-22i16.3*, *ponzr3* and *wu:fj16a03* (Table 1). We were particularly intrigued by Fkbp5, a member of the conserved FK506 binding protein (FKBP) family. The FKBP family consists of a large number of structurally related proteins known for their capability of binding to and modulating the immunosuppressive actions of FK506 as well as rapamycin, a well-known mTOR inhibitor [16]. Rapamycin treatment inhibited NaR cell reactivation and proliferation [7]. Among the 19 zebrafish *fkbp* gene family members (Fig. 2A), the expression of *fkbp5* and *fkbp-like*, but not other *fkbp* genes, was increased in reactivated NaR cells (Fig. 2B). The up-regulation of *fkbp5* mRNA expression was confirmed by qRT-PCR (Fig. 2C). In comparison, the mRNA levels of *fkbp7*, a related member of the Fkbp gene family, showed no change (Fig. 2C).

To determine whether Fkbp5 plays a role in reactivating NaR cells, *Tg(igfbp5a:GFP)* fish were treated with FK506, a pan FKBP inhibitor [17]. FK506 treatment inhibited the induction medium-induced NaR cell proliferation, whereas it did not change the basal NaR cell number in fish kept in the control medium

Table 1. Top up-regulated genes based on mRNA abundance.

Gene name	Known function
<i>col2a1a</i>	Collagen, type II
<i>trpv6</i>	Epithelial calcium channel
<i>caspb</i>	Thiol protease
<i>her9</i>	Predicted to have DNA-binding transcription repressor activity
<i>ankhb</i>	Regulates intra- and extracellular levels of inorganic pyrophosphate
<i>pck1</i>	Phosphoenolpyruvate carboxykinase
<i>fkbp5</i>	Immunophilin protein family member
<i>si:dkey-22i16.3</i>	ncRNA?
<i>ponzr3</i>	Plac8 onzin-related protein 3
<i>wu:fj16a03</i>	?

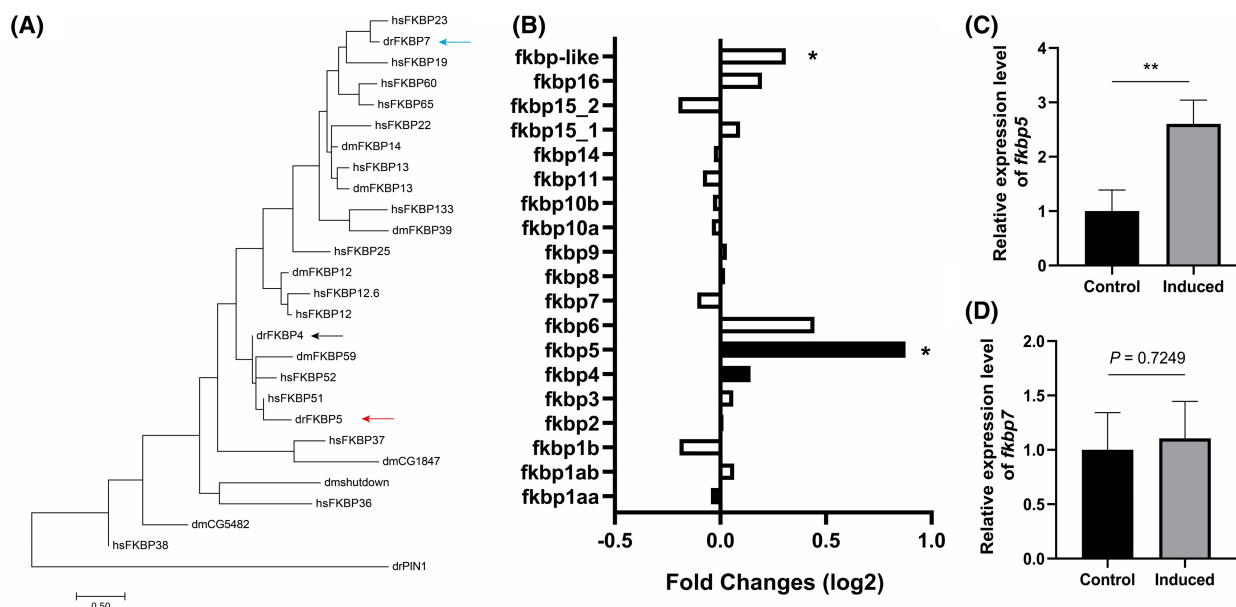


Fig. 2. Up-regulation of *fkbp5* expression in reactivated NaR cells. (A) Phylogenetic tree of humans (hs), zebrafish (dr) and *Drosophila* (dm) FKBP. Pin1 prolyl *cis-trans* isomerase drPIN1 is used as an outgroup. (B) Relative levels of *fkbp* mRNAs detected by RNA-seq. The mRNA levels of the indicated genes in reactivated NaR cells were normalised by those of the control NaR cells. Data shown are mean. * $P < 0.05$. (C) qRT-PCR results. NaR cells were isolated by fluorescence-activated cell sorting as described in Fig. 1. The mRNA level of *fkbp5* (upper panel) and *fkbp7* (lower panel) were detected by qRT-PCR and expressed as fold change over the control group. $n = 4$. Data shown are mean \pm SD. ** indicates $P < 0.01$.

(Fig. 3A,B). Next, a CRISPR-Cas9-based F0 gene deletion approach was used to genetically delete Fkbp5. This method can convert over 90% of injected embryos directly into biallelic knockout [18,19] and is well suited for functional analysis of essential genes. Injection of *fkbp5* targeting gRNAs abolished NaR cell reactivation while scrambled gRNAs had not such an effect (Fig. 3C). Deletion of Fkbp5 did not alter the number of NaR cells under the control medium (Fig. 3C). In comparison, CRISPR/Cas9-mediated knockdown of Fkbp7 had little effect (Fig. 3D). Together, these data suggest that elevated Fkbp5 expression promotes NaR cell quiescence-proliferation transition.

Fkbp5 promotes NaR cell proliferation via Akt signalling

If Fkbp5 acts in the Igf1r-PI3 kinase-Akt pathway to stimulate NaR cell reactivation and proliferation, then deletion of Fkbp5 should alter Akt signalling activity in these cells. Likewise, constitutive activation of Akt should reverse the effects of Fkbp5 inhibition. Indeed, while the induction medium treatment resulted in a robust increase in the number of phosphor-Akt positive cells in un-injected or scrambled gRNA injected fish (Fig. 4A), this effect was impaired by CRISPR/

Cas9-mediated *fkbp5* deletion (Fig. 4B). Next, myrAkt, a constitutively active form of Akt [20], was expressed in a subset of NaR cells using a Tol2 transposon-mediated genetic mosaic assay [21]. While FK506 treatment impaired NaR cell reactivation and proliferation in normal NaR cells, this effect was reversed by myrAkt expressing (Fig. 4C). These data suggest that Fkbp5 promotes NaR cell reactivation and proliferation via Akt signalling.

Discussion

In this study, we used a zebrafish model and mapped transcriptomic changes during epithelial cell quiescence to proliferation transition *in vivo*. Our transcriptomic analysis showed that genes involved in transcription/regulation, cell cycle, Foxo, Wnt and PPAR signalling are increased while those involved in ion transport, cell adhesion and oxidation-reduction are down-regulated in the reactivated cells. These findings support the notion that low calcium stress induces differentiated NaR cells to re-enter the active cell cycle via reactivating the PI3 kinase-Akt pathway [8,9,11]. Further data mining, genetic and biochemical analyses showed that Fkbp5 plays a critical role in stimulating NaR cell proliferation-quiescence transition via Akt signalling.

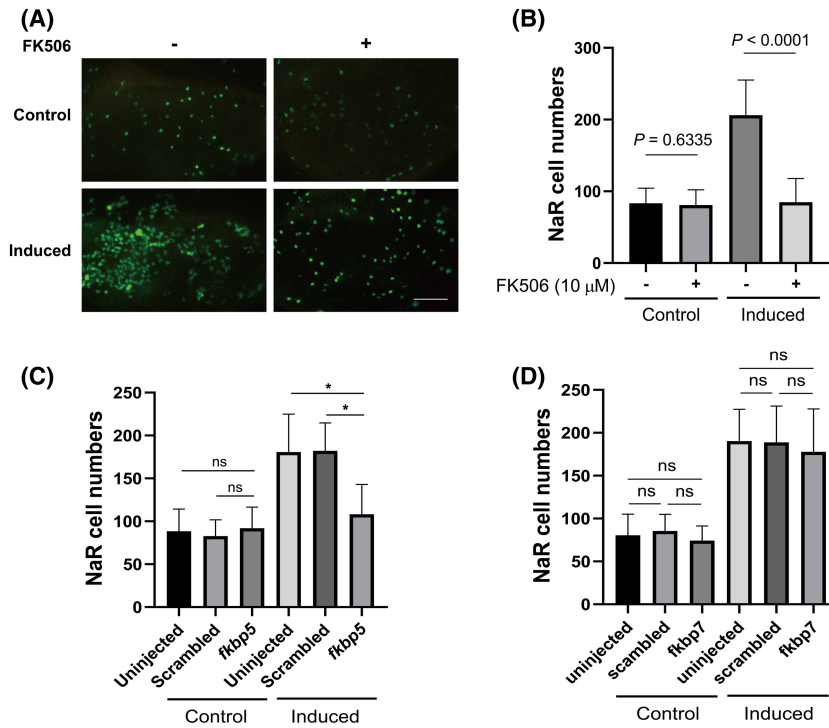


Fig. 3. Fkbp5 promotes NaR cell quiescence-proliferation transition. (A, B) Effect of FK506. *Tg(igfbp5a:GFP)* embryos were raised in E3 medium to 3 dpf and transferred to the control and induction medium with or without 10 μ M FK506. NaR cells were quantified at 5 dpf. Representative images were shown in (A) and quantified data in (B). Scale bar = 0.2 mm. Data shown are mean \pm SD. $n = 37$ –58. (C, D) *Tg(igfbp5a:GFP)* embryos were injected with *Cas9* mRNA and gRNAs targeting *fkbp5* (C), *fkbp7* (D) or scrambled gRNA at the one-cell stage. They were raised in E3 solution to 3 dpf and transferred to the control (Control) or induction medium (induced). NaR cells were quantified 2 days later. Data shown are mean \pm SD. $n = 17$ –69.

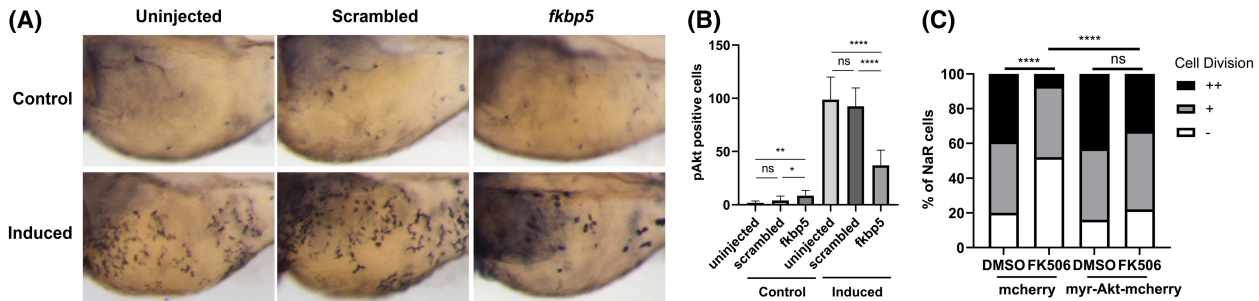


Fig. 4. Fkbp5 promotes NaR cell quiescence-proliferation transition via Akt signalling. (A, B) *Tg(igfbp5a:GFP)* embryos were raised in E3 medium until 3 dpf and transferred to the control (Control) or induction medium (induced). Two days later, they were subjected to phospho-Akt immunostaining. Phospho-Akt-positive cells in the yolk sac region were quantified. Representative images were shown in (A) and quantified data in (B). Data shown are mean \pm SD. (C) Effect of myrAkt expression. *Tg(igfbp5a:GFP)* embryos injected with *BAC(igfbp5a:mCherry)* or *BAC(igfbp5a:myr-Akt-mCherry)* were raised. At 3 dpf, they were transferred to the induction medium containing DMSO or 10 μ M FK506. At 5 dpf, NaR cells labelled by both GFP and mCherry were scored following a previously established scoring system [21]. NaR cells that did not divide, divided one time or two times are scored as -, + and ++, respectively. * $P < 0.05$; **** $P < 0.0001$; ns, not significant. Total cell number is shown above each column.

As expected, a significant enrichment of the cell cycle genes was observed in reactivated and dividing NaR cells. Although p53 signalling and cellular

senescence pathway are also enriched, a close look suggested that many of the enriched genes are overlapping with those in the cell cycle genes (Fig. S3).

GADD45 and CDK1 have been implicated in the modulation of cell cycle and apoptosis in mammalian cells [22]. Likewise, *ccne2*, *ccnd1* and *ccnd2*, which encode Cyclin E2, D1 and B2, are key regulators of cell cycle and frequently overexpressed in cancer cells [23–25]. In zebrafish, *Cdk21* has been shown to promote male germ cell proliferation and meiosis [26]. In addition to cell cycle genes, several DNA repair pathway genes are enriched in the reactivated and proliferation NaR cells. Cell division requires the faithful copying of the genome once per cell cycle. Robust cell replication can lead to replication stress and activates DNA damage repair pathways such as homologous recombination [27]. It is possible that the rapid dividing NaR cells may experience replication stress. This is consistent with the enrichment of Fanconi anaemia genes in these cells. The Fanconi anaemia pathway functions as a DNA damage repair system [28].

In previous studies, we have shown that the reactivation of Akt is required and sufficient in promoting NaR cell reactivation and proliferation [5,7–9]. In this study, many genes in the Foxo signalling pathway are enriched (Fig. S4). A key mechanism in the regulation of FOXO proteins is the phosphorylation by AKT, in response to insulin or IGFs stimulation. This modification promotes FOXO proteins to exit from the nucleus and decreases the expression of the FOXO target genes [29]. Among the DEGs in this pathway are *Sgk1* and *Sgk3*, two Akt-like protein kinases. SGK1 has been reported to be activated by insulin and IGFs via the PDK1 and TORC2 [30,31]. SGK1 increases the protein abundance and/or activity of several ion channels, solute carriers and Na^+/K^+ -ATPases [32]. Overexpression of SGK3 in hepatocellular carcinoma has been shown to increase cell cycle progression through G1 by inactivating glycogen synthase kinase- β and stabilising CCND1 [33]. Future genetic studies are needed to elucidate the possible roles of *Sgk1* and/or *Sgk3* in NaR cell quiescence-proliferation regulation.

Multiple Wnt ligands are enriched in the up-regulated genes in proliferating NaR cells. Wnt signalling plays a crucial role in melanocyte development [15]. In *Xenopus* epidermis, Wnt signalling is required for cilia formation and differentiation of multiciliate epithelial cells. In basal cells, Wnt signalling prevents specification of epithelial cell types via ΔN -TP63, a master transcription factor [34]. NaR cells are located on the yolk sac epidermis in zebrafish embryos and larvae. It will be interesting to determine whether these Wnt ligand genes play a direct role in regulating NaR cell development and proliferation. Another pathway of interest is PPAR signalling. Several genes, including *pck1* and *pck2*, are

enriched in the reactivated NaR cells. While PCK1 is well known as a gluconeogenic enzyme, recent studies show that PCK1 and its mitochondrial counterpart PCK2 also increase TCA cycle flux to stimulate cell proliferation in colon cancer-derived cell lines [35–37]. It is unclear whether any of these PPAR genes plays a role in regulating NaR cell fate.

NaR cells are one of the several types of ionocytes derived from epidermal stem cells [9,10]. NaR cells are polarised cells with an apical opening facing the external environments and basolateral sides facing the internal body fluids. These cells are responsible for transcellular Ca^{2+} transport, which also involves Na^+ and K^+ trafficking [10]. Our transcriptomic analysis showed that the GO term of ‘transport’ was most highly enriched among the down-regulated genes. Out of the 996 down-regulated genes, 57 are in this group. Within this category, 11 genes are known to be involved in ion transport. These include several calcium ion channels, potassium channels and Na^+ , Cl^- and H^+ channels and transporters. The down-regulation of these genes, together with the reduction of cell adhesion genes, supports the notation that NaR cells undergo dedifferentiation and become reactivated. We have previously found that the epithelial calcium channel *trpv6* plays a critical role in stimulating NaR cell quiescence. This study identified three additional calcium channels, including *cacng1a* (calcium channel, voltage-dependent, gamma subunit 1a), *cacng3a* and *trpv1* down-regulated in reactivated NaR cells. *Trpv1* is critical for heat sensing [38]. Currently, little is known about the function of *cacng1a* and *cacng3a*. The roles of these channels in NaR cell quiescence-proliferation balance, if any, are unknown at present and deserves further investigation.

A key finding made in this study is that *Fkbp5* played a critical role in promoting NaR cell quiescence-proliferation transition. This conclusion is supported by several lines of evidence. First, *fkbp5* mRNA expression is up-regulated in reactivated NaR cells. In comparison, the expression of *fkbp7* and many other *fkbp* genes was not changed. Second, pharmacological inhibition of *Fkbp* prevented NaR cell quiescence-proliferation transition. Furthermore, genetic deletion of *Fkbp5* impaired NaR cell reactivation and proliferation. This effect is specific because deletion of *Fkbp7* had little effect. Although a previous study reported that FKBP51 (encoded by the human *FKBP5* gene) promotes the expression of epithelial-to-mesenchymal transition genes [39], a role of *Fkbp5* in cell quiescence-proliferation decision has not been reported. FKBP5 have a variety of molecular masses that are involved in several signal transduction pathways [16,40,41]. Human

FKBP51 was originally discovered as a co-chaperone of Hsp90 and a component of the Hsp90-steroid receptor heterocomplex [42]. FKBP51 contains 2 FKBP domains and 3 tetratricopeptide-repeats domain. While the first FKBP domain (FK1) has [peptidylprolyl isomerase](#) activity and provides a binding pocket for FK506 and [rapamycin](#), FK2 lacks the PPIase activity. Among the FKBP family members, FKBP51 is most closely related to FKBP52 (encoded by the human *FKBP-4* gene) [43]. Despite the high sequence similarity, these two proteins had different and often opposite roles in several biological processes. While one was found to facilitate the dephosphorylation of Akt via the phosphatase PHLPP [44,45], the other had a capability to promote Akt phosphorylation through PI3K/PDK1 and mTORC2 [46]. In this study, we provided genetic evidence that Fkbp5 acts upstream of Akt to promote NaR cell reactivation and proliferation. This conclusion is supported by the fact that CRISPR/Cas9-mediated deletion and pharmacological inhibition of Fkbp5 attenuated Akt signalling in NaR cells while targeted expression of myrAkt 'rescued' FK506 effect on NaR cell reactivation.

As a central node for signal transduction and proliferation, Akt integrated multiple intracellular signalling including Ca^{2+} flux. Intracellular Ca^{2+} /calmodulin signalling has been implicated in Akt activation in cultured mammalian cells [47]. Our recent study showed that ER Ca^{2+} efflux activated Ca^{2+} /calmodulin-dependent protein kinase kinase (CaM-KK), and this in turn activated Akt to induce NaR cell reactivation [11]. Human FKBP 12 and FKBP12.6 are both known to regulate ER Ca^{2+} flux via the association with ER Ca^{2+} channels like ryanodine receptors (RyRs) and inositol 1,4,5-trisphosphate receptors (IP3Rs) [48,49]. Our transcriptomic analysis showed the mRNA levels of *fkbp1aa*, *fkbp1ab* and *fkbp1b*, which encode zebrafish Fkbp12 and Fkbp12.6a and -b, were not significantly changed in reactivated NaR cells. Treatment of zebrafish larvae with RyRs inhibitors ryanodine and dantrolene blocked NaR cell reactivation while the IP3R inhibitor xestospongine C did not have such an effect [11]. Future studies are needed to determine whether Fkbp5 regulates Akt signalling by altering RyRs-mediated ER Ca^{2+} flux in NaR cells.

Materials and methods

Chemicals and reagents

All chemical reagents were purchased from Fisher Scientific (Pittsburgh, PA, USA) unless stated otherwise. Liberase TM was purchased from Sigma-Aldrich (St Louis, MO, USA).

FK506 was purchased from Selleck Chemicals (Houston, TX, USA). Oligonucleotide primers, the TRIzol reagent, Moloney murine leukemia virus (M-MLV) reverse transcriptase and RNaseOUT Recombinant Ribonuclease Inhibitor were purchased from Invitrogen (Carlsbad, CA, USA). The Phospho-Akt (Ser473) antibody was purchased from Cell Signaling Technology (Beverly, MA, USA). The pT3.Cas9-UTRglobin plasmid was a gift from Prof. Yonghua Sun, Institute of Hydrobiology, Chinese Academy of Sciences.

Zebrafish

Zebrafish were raised following standard zebrafish husbandry guidelines [50]. Embryos were obtained by natural cross and staged following Kimmel *et al.* [51]. All embryos were raised in the standard E3 embryo medium [50] until 3 dpf. The control embryo medium (containing 0.2 mM $[\text{Ca}^{2+}]$) and the induction embryo medium (containing 0.001 mM $[\text{Ca}^{2+}]$) were prepared following a previously reported formula [5]. In some experiments, 0.003% (w/v) N-phenylthiourea was added to the media to inhibit pigmentation. The *Tg(igfbp5a:GFP)* fish line was generated in a previous study [7]. All experiments were conducted in accordance with the guidelines approved by the University of Michigan Institutional Committee on the Use and Care of Animals.

FACS, RNA-seq and quantitative real-time PCR (qPCR) analysis

Isolation and sorting of NaR cells by FACS were performed as previously described [7]. For RNA-seq, RNA was isolated from FACS-sorted NaR cells using a RNeasy Micro Kit (Qiagen, Valencia, CA, USA). The integrity of the RNA samples was confirmed using the Agilent Bioanalyzer 2100 with an RNA 6000 Pico Kit (Agilent, Santa Clara, CA, USA). All samples had an RNA Integrity Number of 8 or greater. cDNA libraries were prepared using a SMART-Seq v4 Ultra Low Input RNA Kit (Singulomics, Palo Alto, CA, USA). Briefly, the first-strand cDNA was synthesised, full-length ds cDNA was amplified by LD-PCR. The amplified cDNA was purified using an Agencourt AMPure XP Kit (Beckman Coulter Life Sciences, Indianapolis, IN, USA) and validated using the Agilent 2100 Bioanalyzer (Agilent). An Illumina Library was prepared. Single-end, 50 bp sequencing was performed on the Illumina Hi-Seq 4000 platform. The quality control of raw reads was tested using FastQC. The raw reads were trimmed using the Trimmomatic [52] and filtered. The pre-processed reads were mapped to the genome sequence of zebrafish GRCz10 (GCA_000002035.3) using TopHat and the aligned reads were assembled into transcripts using Cufflinks. The assembled transcripts were merged with the reference annotation (Danio_rerio.Zv9.68) using cuffmerge. The *sva* package in R was used for removing batch effects.

The htseq-count function was used to detect the number of counts in BAM files. Differential expression analysis was performed using WILCOX.TEST in R package. Heatmap of hierarchical clustering was created using the PHEATMAP R package. The CLUSTERPROFILER package in R was used to perform GO and pathway analysis. To validate the RNA-seq results, NaR cells were FACS sorted and RNA isolation was carried out. cDNA was synthesised using Superscript III Reverse Transcriptase. qPCR was performed on an ABI 7500 fast Real-Time PCR system (Applied Biosystems, Foster City, CA, USA) using SYBR Green (Bio-Rad, Hercules, CA, USA). PCR primers are listed in Table S2.

Phylogenetic analysis of the Fkbp protein family

Phylogenetic tree of the FKBP family in humans (hs), zebrafish (dr) and *Drosophila* (dm) was constructed using the Maximum Likelihood method based on the JTT matrix-based model [53]. The tree was constructed using MEGA7 [54].

Drug treatment

Drugs used in this study were dissolved in DMSO and further diluted in water. Drug treatments began at 3 dpf. The fish were subjected to immunostaining after 1 day treatment or NaR cell quantification after 2 days of treatment.

NaR cell measurement

Tg(igfbp5a:GFP) larvae were imaged under a Leica MZ16F stereo microscope (Leica, Hamburg, Germany) equipped with a QICAM 12-bit Mono Fast 1394 Cooled camera (QImaging, Surry, BC, Canada). Lateral view images were taken and GFP-positive NaR cells were quantified as described [7].

CRISPR/Cas9-mediated F0 gene deletion

Four sgRNAs were used to perform transient deletion of *fkbp5* and *fkbp7* following [19]. The sgRNAs were synthesised by *in vitro* transcription based on a published method [55]. Cas9 mRNA was synthesised by *in vitro* transcription using the pT3.Cas9-UTRglobin plasmid as template. sgRNAs ($40 \text{ ng}\cdot\mu\text{L}^{-1}$) were mixed with Cas9 mRNA ($400 \text{ ng}\cdot\mu\text{L}^{-1}$) and co-injected into *Tg(igfbp5a:GFP)* embryos at one cell stage. The injected embryos were raised in E3 embryo medium. To induce NaR cell reactivation, fish were transferred to the control and induction embryo medium at 3 dpf as previously reported [7]. Knockout efficiency was validated using headloop PCR following ([18,19]).

Tol2 transposon-mediated transgenesis assay

A Tol2 transposon-mediated genetic mosaic assay was used to target the expression of a transgene in a subset of NaR

cells [21]. *BAC(igfbp5a:myrAkt-mCherry)* DNA and Tol2 mRNA were mixed and injected into 1-cell stage *Tg(igfbp5a:GFP)* embryos. The embryos were raised and subjected to various treatments. Cells co-expressing mCherry and GFP were identified, and the cell proliferation index was determined as previously reported [21].

Whole-mount immunostaining

Zebrafish larvae were fixed in 4% paraformaldehyde, permeabilised in methanol and subjected to whole mount immunostaining of phosphor-Akt as described previously [5].

Statistical analysis

Statistical analyses were performed in consultation with the University of Michigan's Consulting for Statistics, Computing and Analytics Research (CSCAR) team. Cell proliferation index data were analysed using pairwise Chi-square tests. Data are shown as mean \pm standard deviation (SD). Statistical analyses between two groups were performed using unpaired two-tailed *t* test. When comparing the means of multiple groups to a control group, Dunnett's test was used to correct for multiple comparisons after one-way ANOVA. Statistical significances from all tests were accepted at $P < 0.05$ or higher.

Funding

This work was supported by NSF IOS-1755268 to CD. The funders had no role in study design, data collection and analysis, decision to publish, or preparation of the manuscript.

Author contributions

CD, CL, and YL performed the conceptualization. YL, CL, and XB involved in investigation. YL and CL performed the visualization. CD and ML involved in supervision. CD, YL, and CL wrote the original draft. YL, CL, XB, M, and CD involved in review and editing.

Peer review

The peer review history for this article is available at <https://www.webofscience.com/api/gateway/wos/peer-review/10.1002/1873-3468.14670>.

Data availability

The data that support the findings of this study are openly available in Table S1 and Data S1–S4.

References

- Pennycook BR and Barr AR (2020) Restriction point regulation at the crossroads between quiescence and cell proliferation. *FEBS Lett* **594**, 2046–2060.
- Pardee AB (1974) A restriction point for control of normal animal cell proliferation. *Proc Natl Acad Sci USA* **71**, 1286–1290.
- Yao G, Lee TJ, Mori S, Nevins JR and You L (2008) A bistable Rb–E2F switch underlies the restriction point. *Nat Cell Biol* **10**, 476–482.
- Spencer SL, Cappell SD, Tsai F-C, Overton KW, Wang CL and Meyer T (2013) The proliferation-quiescence decision is controlled by a bifurcation in CDK2 activity at mitotic exit. *Cell* **155**, 369–383.
- Dai W, Bai Y, Hebda L, Zhong X, Liu J, Kao J and Duan C (2014) Calcium deficiency-induced and TRP channel-regulated IGF1R-PI3K-Akt signaling regulates abnormal epithelial cell proliferation. *Cell Death Differ* **21**, 568–581.
- Li S, Liu C, Goldstein A, Xin Y, Ke C and Duan C (2021) Calcium state-dependent regulation of epithelial cell quiescence by stanniocalcin 1a. *Front Cell Dev Biol* **9**, 662915.
- Liu C, Dai W, Bai Y, Chi C, Xin Y, He G, Mai K and Duan C (2017) Development of a whole organism platform for phenotype-based analysis of IGF1R-PI3K-Akt-tor action. *Sci Rep* **7**, 1–15.
- Liu C, Li S, Noer PR, Kjaer-Sorensen K, Juhl AK, Goldstein A, Ke C, Oxvig C and Duan C (2020) The metalloproteinase Papp-aa controls epithelial cell quiescence-proliferation transition. *Elife* **9**, e52322.
- Xin Y, Malick A, Hu M, Liu C, Batah H, Xu H and Duan C (2019) Cell-autonomous regulation of epithelial cell quiescence by calcium channel Trpv6. *Elife* **8**, e48003.
- Hwang P-P (2009) Ion uptake and acid secretion in zebrafish (*Danio rerio*). *J Exp Biol* **212**, 1745–1752.
- Xin Y, Guan J, Li Y and Duan C (2021) Regulation of cell quiescence–proliferation balance by Ca²⁺–CaMKK–Akt signaling. *J Cell Sci* **134**, jcs253807.
- Chen BC, Wu WT, Ho FM and Lin WW (2002) Inhibition of interleukin-1beta -induced NF-kappa B activation by calcium/calmodulin-dependent protein kinase kinase occurs through Akt activation associated with interleukin-1 receptor-associated kinase phosphorylation and uncoupling of MyD88. *J Biol Chem* **277**, 24169–24179.
- Kim J and Guan KL (2019) mTOR as a central hub of nutrient signalling and cell growth. *Nat Cell Biol* **21**, 63–71.
- Meng D, Frank AR and Jewell JL (2018) mTOR signaling in stem and progenitor cells. *Development* **145**, dev152595.
- Vibert L, Aquino G, Gehring I, Subkankulova T, Schilling TF, Rocco A and Kelsh RN (2017) An ongoing role for Wnt signaling in differentiating melanocytes in vivo. *Pigment Cell Melanoma Res* **30**, 219–232.
- Tong M and Jiang Y (2016) FK506-binding proteins and their diverse functions. *Curr Mol Pharmacol* **9**, 48–65.
- Yeh W-C, Bierer BE and McKnight SL (1995) Rapamycin inhibits clonal expansion and adipogenic differentiation of 3T3-L1 cells. *Proc Natl Acad Sci USA* **92**, 11086–11090.
- Kroll F, Powell GT, Ghosh M, Gestri G, Antinucci P, Hearn TJ, Tunbak H, Lim S, Dennis HW and Fernandez JM (2021) A simple and effective F0 knockout method for rapid screening of behaviour and other complex phenotypes. *Elife* **10**, e59683.
- Wu RS, Lam II, Clay H, Duong DN, Deo RC and Coughlin SR (2018) A rapid method for directed gene knockout for screening in G0 zebrafish. *Dev Cell* **46**, 112–125.e4.
- Kohn AD, Takeuchi F and Roth RA (1996) Akt, a pleckstrin homology domain containing kinase, is activated primarily by phosphorylation. *J Biol Chem* **271**, 21920–21926.
- Liu C, Xin Y, Bai Y, Lewin G, He G, Mai K and Duan C (2018) Ca²⁺ concentration-dependent premature death of igfbp5a^{-/-} fish reveals a critical role of IGF signaling in adaptive epithelial growth. *Sci Signal* **11**, eaat2231.
- Kleinsimon S, Longmuss E, Rolff J, Jäger S, Eggert A, Delebinski C and Seifert G (2018) GADD45A and CDKN1A are involved in apoptosis and cell cycle modulatory effects of viscumTT with further inactivation of the STAT3 pathway. *Sci Rep* **8**, 1–14.
- Fu M, Wang C, Li Z, Sakamaki T and Pestell RG (2004) Minireview: cyclin D1: normal and abnormal functions. *Endocrinology* **145**, 5439–5447.
- Joo M, Kang YK, Kim MR, Lee HK and Jang JJ (2001) Cyclin D1 overexpression in hepatocellular carcinoma. *Liver* **21**, 89–95.
- Nagasawa S, Onda M, Sasajima K, Makino H, Yamashita K, Takubo K and Miyashita M (2001) Cyclin D1 overexpression as a prognostic factor in patients with esophageal carcinoma. *J Surg Oncol* **78**, 208–214.
- Webster KA, Henke K, Ingalls DM, Nahrin A, Harris MP and Siegfried KR (2019) Cyclin-dependent kinase 21 is a novel regulator of proliferation and meiosis in the male germ line of zebrafish. *Reproduction* **157**, 383–398.
- Gaillard H, García-Muse T and Aguilera A (2015) Replication stress and cancer. *Nat Rev Cancer* **15**, 276–289.
- Datta A and Brosh RM Jr (2019) Holding all the cards-how Fanconi anemia proteins deal with replication stress and preserve genomic stability. *Genes* **10**, 170.

- 29 Manning BD and Cantley LC (2007) AKT/PKB signaling: navigating downstream. *Cell* **129**, 1261–1274.
- 30 Castel P, Ellis H, Bago R, Toska E, Razavi P, Carmona FJ, Kannan S, Verma CS, Dickler M and Chandarlapaty S (2016) PDK1-SGK1 signaling sustains AKT-independent mTORC1 activation and confers resistance to PI3K α inhibition. *Cancer Cell* **30**, 229–242.
- 31 Zhou B, Zhang Y, Li S, Wu L, Fejes-Toth G, Naray-Fejes-Toth A and Soukas AA (2021) Serum-and glucocorticoid-induced kinase drives hepatic insulin resistance by directly inhibiting AMP-activated protein kinase. *Cell Rep* **37**, 109785.
- 32 Lang F and Shumilina E (2013) Regulation of ion channels by the serum- and glucocorticoid-inducible kinase SGK1. *FASEB J* **27**, 3–12.
- 33 Hou M, Lai Y, He S, He W, Shen H and Ke Z (2015) SGK3 (CISK) may induce tumor angiogenesis (hypothesis). *Oncol Lett* **10**, 23–26.
- 34 Haas M, Vázquez JLG, Sun DI, Tran HT, Brislinger M, Tasca A, Shomroni O, Vleminckx K and Walentek P (2019) Δ N-Tp63 mediates Wnt/ β -catenin-induced inhibition of differentiation in basal stem cells of mucociliary epithelia. *Cell Rep* **28**, 3338–3352.e6.
- 35 Balsa-Martinez E and Puigserver P (2015) Cancer cells hijack gluconeogenic enzymes to fuel cell growth. *Mol Cell* **60**, 509–511.
- 36 Montal ED, Dewi R, Bhalla K, Ou L, Hwang BJ, Ropell AE, Gordon C, Liu W-J, DeBerardinis RJ and Sudderth J (2015) PEPCK coordinates the regulation of central carbon metabolism to promote cancer cell growth. *Mol Cell* **60**, 571–583.
- 37 Vincent EE, Sergushichev A, Griss T, Gingras M-C, Samborska B, Ntimbane T, Coelho PP, Blagih J, Raissi TC and Choinière L (2015) Mitochondrial phosphoenolpyruvate carboxykinase regulates metabolic adaptation and enables glucose-independent tumor growth. *Mol Cell* **60**, 195–207.
- 38 Gau P, Poon J, Ufret-Vincenty C, Snelson CD, Gordon SE, Raible DW and Dhaka A (2013) The zebrafish ortholog of TRPV1 is required for heat-induced locomotion. *J Neurosci* **33**, 5249–5260.
- 39 Romano S, Staibano S, Greco A, Brunetti A, Nappo G, Ilardi G, Martinelli R, Sorrentino A, Di Pace A and Mascolo M (2013) FK506 binding protein 51 positively regulates melanoma stemness and metastatic potential. *Cell Death Dis* **4**, e578.
- 40 Boonying W, Joselin A, Huang E, Qu D, Safarpour F, Iyirhiaro GO, Gonzalez YR, Callaghan SM, Slack RS and Figeys D (2019) Pink1 regulates FKBP 5 interaction with AKT/PHLPP and protects neurons from neurotoxin stress induced by MPP+. *J Neurochem* **150**, 312–329.
- 41 Somarelli J, Lee S, Skolnick J and Herrera R (2008) Structure-based classification of 45 FK506-binding proteins. *Proteins* **72**, 197–208.
- 42 Smith DF, Sullivan WP, Marion TN, Zaitso K, Madden B, McCormick DJ and Toft DO (1993) Identification of a 60-kilodalton stress-related protein, p60, which interacts with hsp90 and hsp70. *Mol Cell Biol* **13**, 869–876.
- 43 Wang L (2011) FKBP51 regulation of AKT/protein kinase B phosphorylation. *Curr Opin Pharmacol* **11**, 360–364.
- 44 Hou J and Wang L (2012) FKBP5 as a selection biomarker for gemcitabine and Akt inhibitors in treatment of pancreatic cancer. *PLoS One* **7**, e36252.
- 45 Pei H, Li L, Fridley BL, Jenkins GD, Kalari KR, Lingle W, Petersen G, Lou Z and Wang L (2009) FKBP51 affects cancer cell response to chemotherapy by negatively regulating Akt. *Cancer Cell* **16**, 259–266.
- 46 Mangé A, Coyaud E, Desmetz C, Laurent E, Béganton B, Coopman P, Raught B and Solassol J (2019) FKBP4 connects mTORC2 and PI3K to activate the PDK1/Akt-dependent cell proliferation signaling in breast cancer. *Theranostics* **9**, 7003–7015.
- 47 Deb TB, Coticchia CM and Dickson RB (2004) Calmodulin-mediated activation of Akt regulates survival of c-Myc-overexpressing mouse mammary carcinoma cells. *J Biol Chem* **279**, 38903–38911.
- 48 Gonano LA and Jones PP (2017) FK506-binding proteins 12 and 12.6 (FKBPs) as regulators of cardiac ryanodine receptors: insights from new functional and structural knowledge. *Channels* **11**, 415–425.
- 49 MacMillan D (2013) FK506 binding proteins: cellular regulators of intracellular Ca²⁺ signalling. *Eur J Pharmacol* **700**, 181–193.
- 50 Westerfield M (2000) *The Zebrafish Book. A Guide for the Laboratory Use of Zebrafish (Danio rerio)*. 4th edn. Eugene, University of Oregon Press.
- 51 Kimmel CB, Ballard WW, Kimmel SR, Ullmann B and Schilling TF (1995) Stages of embryonic development of the zebrafish. *Dev Dyn* **203**, 253–310.
- 52 Bolger AM, Lohse M and Usadel B (2014) Trimmomatic: a flexible trimmer for Illumina sequence data. *Bioinformatics* **30**, 2114–2120.
- 53 Jones DT, Taylor WR and Thornton JM (1992) The rapid generation of mutation data matrices from protein sequences. *Bioinformatics* **8**, 275–282.
- 54 Kumar S, Stecher G and Tamura K (2016) MEGA7: molecular evolutionary genetics analysis version 7.0 for bigger datasets. *Mol Biol Evol* **33**, 1870–1874.
- 55 Shao Y, Guan Y, Wang L, Qiu Z, Liu M, Chen Y, Wu L, Li Y, Ma X and Liu M (2014) CRISPR/Cas-mediated genome editing in the rat via direct injection of one-cell embryos. *Nat Protoc* **9**, 2493–2512.

Supporting information

Additional supporting information may be found online in the Supporting Information section at the end of the article.

Fig. S1. RNA-seq data quality. (A) Percentage of read mapping. (B) Distribution of count values for genes expressed in the four control (C) and four induction groups (I) of NaR cells. (C) Correlation coefficient analysis. Values show squared Pearson correlation (R^2). (D) Principal component analysis (PCA) plot of the control (C) and induction groups of cells. Principal component 1 (PC1) and principal component 2 (PC2) were used for analysis.

Fig. S2. Changes in gene expression. NaR cells were isolated by FACS sorting as described in Fig. 1A. The mRNA levels of the indicated genes were measured by qPCR (blue) or RNA-seq (green) and shown as the ratio between the induction groups and the control groups.

Fig. S3. Heatmaps of enriched genes in cell cycle (A), p53 pathway (B) and cellular senescence (C) in the four control (C1-C4) and induction (R1-R4) groups of cells. Note the significant overlaps in these 3 categories.

Fig. S4. Heatmap of enriched genes in the Foxo signalling pathway in the four control (C1-C4) and four induction (R1-R4) groups of NaR cells.

Fig. S5. Heatmaps of enriched genes in Wnt signalling (A) and melanogenesis (B) pathway in the four control (C1-C4) and four induction (R1-R4) groups of NaR cells. Note the significant overlap in EDGs in these 2 categories.

Fig. S6. Heatmaps of enriched genes in the PAAR signalling (A) and Fanconi anaemia pathway (B) in the four control (C1-C4) and four induction (R1-R4) groups of NaR cells.

Table S1. Significant regulated genes.

Table S2. Genes and primers used in qPCR.

Data S1. Supplemental data - Figure 1E.

Data S2. Supplemental data - Figure 2.

Data S3. Supplemental data - Figure 3.

Data S4. Supplemental data - Figure 4.